



Growth of gallium nitride on silicon by molecular beam epitaxy incorporating a chromium nitride interlayer

Kuang-Wei Liu^a, Sheng-Joue Young^{b,*}, Shoou-Jinn Chang^{a,c,**}, Tao-Hung Hsueh^a, Hung Hung^c, Shi-Xiang Chen^c, Yue-Zhang Chen^d

^a Institute of Electro-Optical Science and Engineering, National Cheng Kung University, Tainan 701, Taiwan

^b Department of Electronic Engineering, National Formosa University, Huwei, Yunlin 632, Taiwan

^c Institute of Microelectronics and Department of Electrical Engineering, Center for Micro/Nano Science and Technology, Advanced Optoelectronic Technology Center, National Cheng Kung University, Tainan 701, Taiwan

^d Institute of Nanotechnology and Microsystems Engineering, National Cheng Kung University, Tainan 701, Taiwan

ARTICLE INFO

Article history:

Received 14 March 2011

Received in revised form 19 June 2011

Accepted 5 August 2011

Available online 27 August 2011

Keywords:

GaN

CrN

MBE

ABSTRACT

This study grew GaN epilayers on Si(111) substrate via molecular beam epitaxy, with a CrN interlayer fabricated through a nitridation process. The X-ray diffraction results showed two peaks corresponding to CrN(111) and GaN(002). The results of auger electron spectroscopy showed that the concentration of electrons was relatively low in the samples grown with a CrN interlayer, due to CrN preventing Si atoms from diffusing into the GaN epilayer, thereby reducing electron concentration. Photoluminescence spectra indicated that donor–acceptor pair recombination (DAP) emission was not generated in the GaN with a CrN interlayer because of improved crystalline quality and a reduction in electron concentration.

© 2011 Elsevier B.V. All rights reserved.

1. Introduction

Gallium nitride (GaN)-based compound semiconductors have been widely utilized in optoelectronic devices, due to their wide energy band-gap (~3.4 eV) and excellent chemical and thermal stability [1]. A sapphire substrate is usually employed for the growth of GaN-based LEDs, though silicon substrates have a number of attractive advantages compared to sapphire substrates, including good thermal and electrical conductivity, low-cost production, and well-developed fabrication processes. Optoelectronic devices including LEDs [2,3], photo detectors [4], and field-effect transistors [5] based on III-nitride have been grown on Si substrates. Unfortunately, a lattice mismatch between GaN and Si substrates can be as high as 17%, resulting in cracks or dislocations in GaN epilayers [6]. Therefore, a low-temperature GaN or AlN layer is generally used as a buffer layer [7,8] or a lateral over growth [9] to reduce cracks and dislocation density.

CrN has recently been used as an interlayer for GaN-based vertical-LEDs fabricated in a chemical lift-off (CLO) process [10].

Because of their notable chemical and thermal stability, CrN films can be fabricated via a nitridation process with Cr thin films, RF co-sputtering deposition, and co-evaporating in nitrogen plasma-assisted molecular beam epitaxial (MBE) systems [11–13]. CrN grown on c-sapphire or AlN/c-sapphire substrates have been shown to follow the orientation of CrN (111) [13,14]. The orientation of GaN layers grown on CrN (111) buffer layers has been demonstrated to follow the c-axis [12]. Improvements in crystalline quality and a reduction in threading dislocation have also been reported regarding MBE-grown GaN on sapphire substrates with CrN buffers [13]. Nevertheless, studies are scant regarding GaN films grown on Si substrates with CrN interlayers. Therefore, this study proposed utilizing the properties of CrN to overcome the mismatches in the lattices of GaN and Si substrates, thereby reducing the density of associated dislocations. The research involved forming CrN by implementing a nitridation process, subsequently growing GaN films on Si substrates with CrN interlayers via MBE. This study also investigated the structural and optical properties of GaN with and without a CrN interlayer.

2. Experiment

In this study, epitaxial layers were grown on a n-type Si substrate with (111) orientation by employing a plasma-assisted MBE system. Initially, a layer of Cr 20 nm in thickness was deposited on the substrate by radio frequency sputtering at room temperature. The Cr-coated Si substrates were subsequently placed into the MBE system at a background pressure of 1.8×10^{-9} Torr. Prior to the growth of GaN epilayers, the Cr-coated Si substrates were treated with nitrogen plasma, which was

* Corresponding author. Tel.: +886 5 6315560; fax: +886 5 6315643.

** Corresponding author at: Institute of Microelectronics and Department of Electrical Engineering, National Cheng Kung University, Tainan 701, Taiwan.

E-mail addresses: shengjoueyoung@gmail.com (S.-J. Young), changsj@mail.ncku.edu.tw (S.-J. Chang).

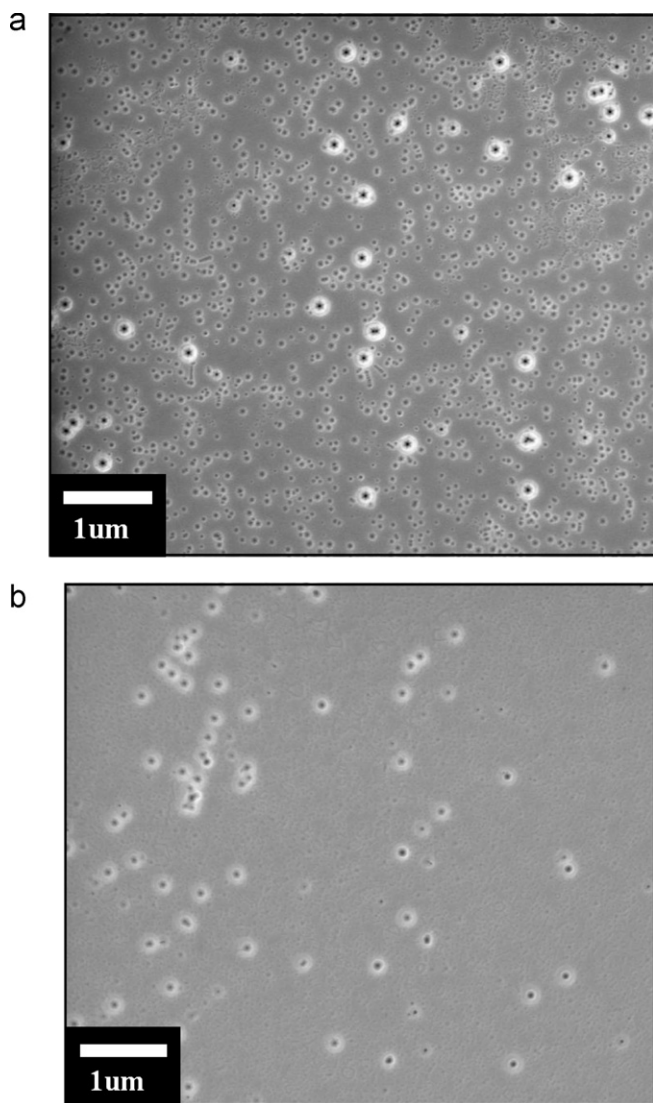


Fig. 1. The plan view SEM image of etched (a) sample without CrN (b) sample with CrN.

generated by supplying high-purity N_2 (99.999% purity) gas at a flow rate of 1.1 sccm and a discharge power of 350 W at 450 °C. A GaN buffer layer (~20 nm) was grown at a temperature of 600 °C in gallium-rich conditions, with a typical growth rate of 210 nm/h. The GaN epilayers were successively grown at a substrate temperature of 700 °C for 2 h, at an estimated growth rate of approximately 300 nm/h. Surface changes of all the samples were monitored by in situ RHEED during growth along the [0002] azimuth.

3. Result and discussion

Fig. 1(a and b) shows scanning electron microscope (SEM) images of the etched GaN with and without CrN interlayer, respectively. During etching pit dislocation (EPD) measurements, we immersed the samples in H_3PO_4 at 160 °C for 3 min. It can clearly be seen that numerous dark pits exist on the surface of both samples. From these two images, it was found that the dark pit density in sample with a conventional LT-GaN buffer was around $3.22 \times 10^{11} \text{ cm}^{-2}$. In contrast, the dark pit density in sample with a CrN interlayer buffer was only around $2.36 \times 10^9 \text{ cm}^{-2}$, the much smaller EPD observed from sample with GaN interlayer indicates that we can indeed reduce the TD density by using the CrN interlayer.

Fig. 2(a) shows the XRD θ - 2θ scan of the GaN grown with and without a CrN interlayer, in which both samples demonstrated

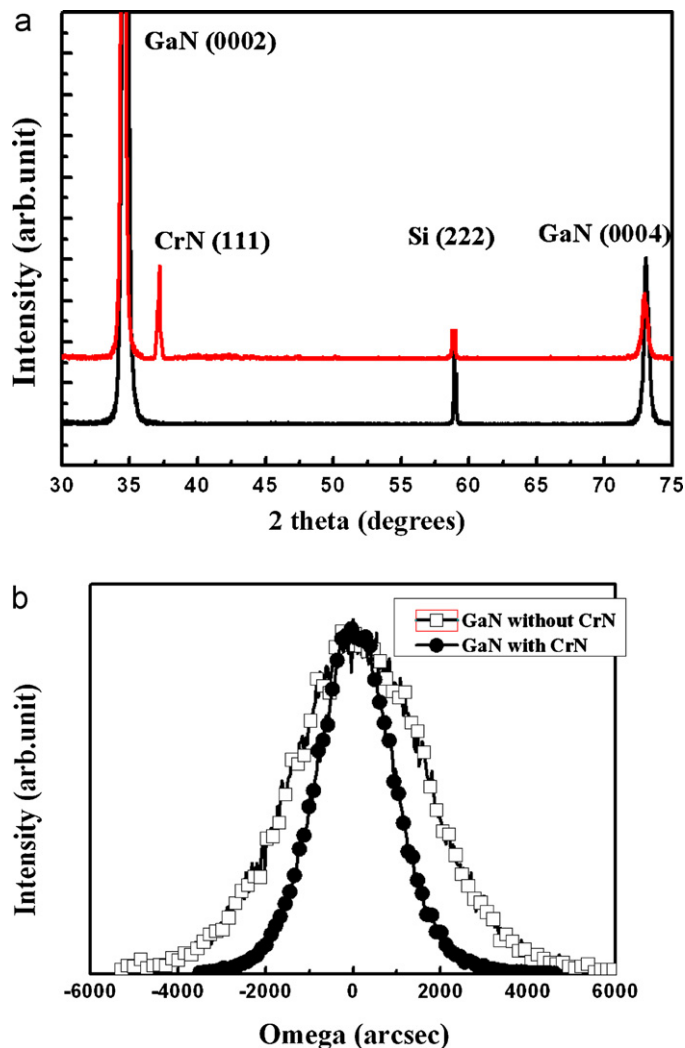


Fig. 2. (a) XRD θ - 2θ scan spectra for the MBE-grown GaN samples with and without a CrN interlayer. GaN (0002) was grown on Si with and without a CrN interlayer. (b) XRC results for the MBE-grown GaN samples with and without a CrN interlayer. The FWHM values of GaN (0002) with and without CrN interlayer were 1833 arc sec and 2808 arc sec, respectively.

major 2θ peaks at 34.54°, 37.12°, 58.83°, and 72.97°, originating from GaN(0002), CrN(111), Si(222), and GaN(0004), respectively [15]. This on-axis θ - 2θ scan indicates that the surface orientation was $(0002)_{\text{GaN}} \parallel (111)_{\text{Si}}$ and $(0002)_{\text{GaN}} \parallel (111)_{\text{CrN}} \parallel (111)_{\text{Si}}$ for the samples with and without CrN interlayers, respectively. Fig. 2(b) shows the X-ray rocking curve (XRC) for GaN(0002) samples. The full-width half maximum (FWHM) values of the rocking curve for the GaN grown with and without the CrN interlayer were 2808 arcsec and 1833 arcsec, respectively. The broadening of the FWHM values was indicative of a defective structure with large edge-threading dislocation in the GaN grown without a CrN interlayer.

Fig. 2(a and b) shows the results of TEM for the sample with the CrN interlayer along the [0001] and $[10\bar{1}0]$ zone axis, respectively. Fig. 3(a) shows a cross-sectional TEM image of GaN grown on a CrN interlayer and Si. The threading dislocation was concentrated in specific regions, as shown in Fig. 3(a) by the arrows. Fig. 3(b) displays the interface between the GaN and Si on the CrN nano-island. The inset shows a fast Fourier transform (FFT) pattern of the CrN nano-island, in which a pattern displays the cubic structure and direction of growth along the (111) direction, the result of FFT corresponds to that of the XRD. According to the TEM and

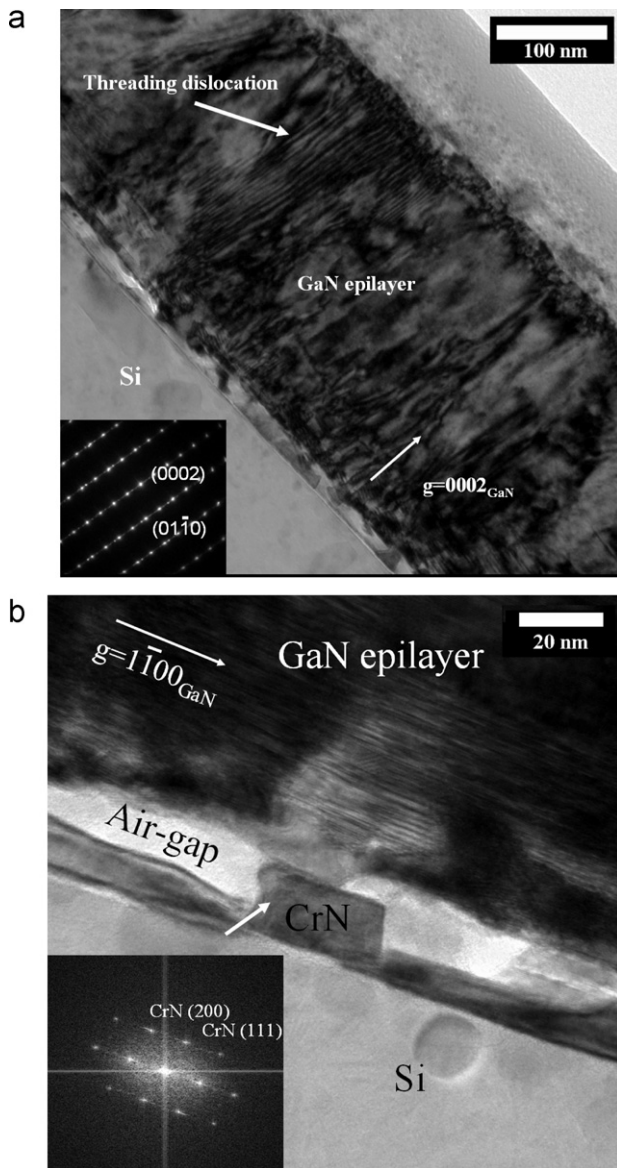


Fig. 3. TEM result of (a) epi-layer and substrate (b) interface for GaN on Si with CrN interlayer, (a) places indicated by the arrow was dislocated from the substrate surface, extending to the epitaxial layer. Insets of (a and b) show the SAED pattern and FFT pattern, these pattern indicated that GaN was grown along c -axis and CrN was a cubic structure which grown along $(1\ 1\ 1)$ direction.

XRD results, the in-plane epitaxial relationship were $(0002)_{\text{GaN}} \parallel (1\ 1\ 1)_{\text{CrN}} \parallel (1\ 1\ 1)_{\text{Si}}$ and $(2\ \bar{1}\ \bar{1}\ 0)_{\text{GaN}} \parallel (0\ 1\ 1)_{\text{CrN}} \parallel (1\ 0\ \bar{1})_{\text{Si}}$ for the samples with the CrN interlayer. An apparent air-gap was found in the interfacial region of the GaN and Si substrate without the CrN nano-island because the lateral growth rate was higher in Ga-rich and high-temperature conditions. Additionally, CrN nano-islands formed in the substrate as nucleation sites during the GaN epitaxial layer growth process, and the grains of the GaN bonded above the area without the CrN nano-island. In this manner, air-gaps were formed beneath the grain boundary, which reduced the density of dislocations in the pattern of the sapphire substrate (PPS) [16].

Hall measurements indicated that the carrier concentrations of the samples, which had been grown with and without CrN interlayers, were $7.72 \times 10^{18}\ \text{cm}^{-3}$ and $1.65 \times 10^{20}\ \text{cm}^{-3}$, respectively. The GaN epilayer without the CrN was diffused by the Si substrate for several hours at a high temperature and low pressure. However, the resulting chemical and thermal stability of the CrN, which

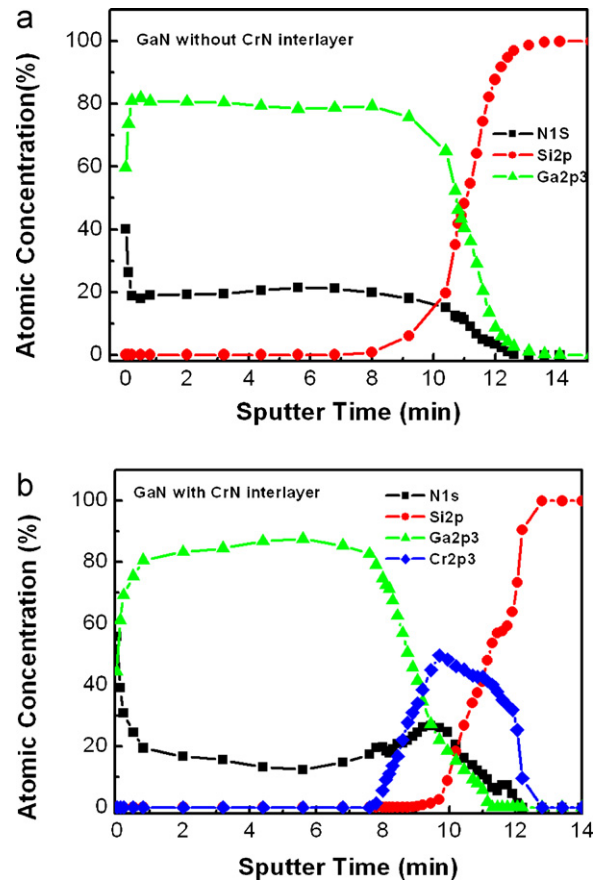


Fig. 4. AES results of GaN (a) without (b) with CrN interlayer. (a) The interface of GaN and Si was contaminated by diffused Si, (b) the CrN interlayer acted as a blocking layer to prevent the Si from diffusing into the GaN epilayer.

prevented the Si from diffusing to the GaN epilayer, caused unintended doping. In addition, the CrN interlayer not only improved the crystalline quality, but also reduced electron concentration in the GaN epilayers. Nevertheless, conducting longitudinal element analysis was possible to confirm the diffusion of Si via Auger electron spectroscopy (AES).

Fig. 3(a and b) shows the AES results of the GaN grown on the Si substrate with and without a CrN interlayer, respectively. The sample grown without a CrN interlayer displayed more Si atoms diffusing into the GaN epilayer compared to the sample grown with a CrN interlayer. This indicates that the CrN interlayer played a role in obstructing the diffusion of Si atoms from the substrate during GaN growth. In addition, Si diffusion into the GaN layers could be the cause of higher carrier concentrations in the GaN grown without a CrN interlayer compared to the GaN grown with a CrN interlayer, on the other hand, in the initial epitaxy state, the quality of GaN was reduced by Si unintended doping, the poor quality of initial epilayer resulted the reduction of GaN epilayer quality, in contrast, the CrN interlayer obstructing Si diffused into GaN initial epilayer to avoid the quality of GaN epilayer was decreased (Fig. 4).

Fig. 5 shows the PL spectra of samples grown with and without CrN interlayer. Fig. 5 shows two peaks located at 365 nm and 380 nm for the GaN sample without a CrN interlayer. The unintended doping caused by Si diffusion into the GaN produced this change in the photoluminescence spectra. The difference in energy between the band-to-band emission (365 nm) and the 380 nm was 169 meV, which was higher than the ionizing energy of Si_{Ga} (27 meV). Because the peak at 380 nm was not donor-to-valence band photoluminescence, this may have been a result of the donor-to-acceptor transition [17]. This is due to Ga vacancy being the

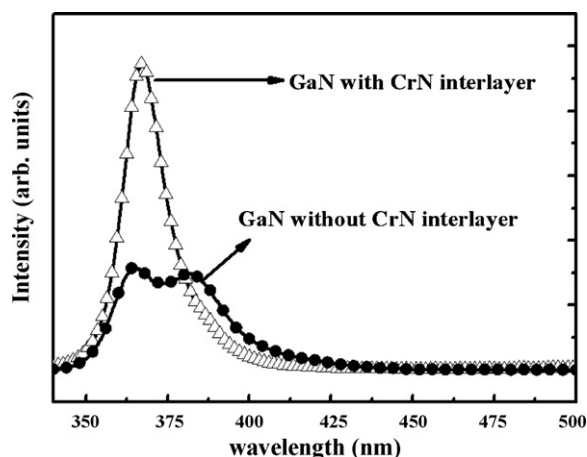


Fig. 5. Photoluminescence spectra of the MBE-grown GaN samples with and without a CrN interlayer. The peak located at 368 nm for GaN with CrN interlayer and two peaks located at 365 nm and 380 nm for GaN without CrN interlayer. Due to CrN as a blocking layer to prevent Si diffused into GaN epilayer, the 380 nm of the peak does not appear in GaN with CrN interlayer.

dominant native defect in the n-type doping (or unintended doping) conditions, acting as an acceptor [18]. GaN with a CrN interlayer displayed only one peak at 368 nm, which may have been due to the prevention of Si diffusion by the CrN interlayer. Thus, the CrN layer seemingly prevents Si from diffusing into the GaN epilayer from the Si substrate, thereby reducing electron concentration, reducing Ga vacancies, and improving crystalline quality. The sample without a CrN interlayer demonstrated a lower degree of integral PL intensity and wider FWHM compared the sample with a CrN interlayer, which implies that the CrN interlayer improved the crystalline quality of the grown GaN epilayer.

4. Conclusion

In summation, this study grew a GaN epilayer on an Si(111) substrate with a CrN interlayer formed by the nitridation of a sputter-coated Cr metal film. The GaN epilayer displayed a crystal orientation of [0002], and the EPD measurement and XRC results demonstrated that the growth of a CrN interlayer between the Si substrate and the GaN epilayer reduces dislocation density and increases crystalline quality. The TEM results also confirmed that CrN reduced the number of dislocations such as pattern sapphire substrates do. In the sample with the CrN interlayer, electron concentration was reduced 100-fold compared with the GaN grown without CrN. Photoluminescent spectra indicated donor-to-acceptor transition in the GaN films grown without a CrN

interlayer, which may have been caused by a diffusion of Si atoms from the Si substrate. The unintended doping of Si resulted in Ga vacancies being recognized as an acceptor material. The PL intensity and FWHM of the band-edge emission were improved in the GaN film grown with a CrN interlayer. This effect can be attributed to the prevention of Si diffusion by the CrN interlayer, which consequently reduced Ga vacancy and improved the crystallinity of the grown GaN epilayer. The results of this study show that a CrN interlayer is significant for the growth of GaN epilayers.

Acknowledgments

This work was supported by National Science Council of Taiwan under Contract numbers NSC 100-2221-E-150-057, NSC 99-2218-E-150-003 and NSC 99-2622-E-150-012-CC3. National Formosa University Research and Services Headquarters that provided the partial equipment for measurement is also acknowledged.

This work was also supported in part by the Center for Frontier Materials and Micro/Nano Science and Technology, National Cheng Kung University (NCKU), Taiwan (D97-2700), and in part by the Advanced Optoelectronic Technology Center, NCKU, under projects from the Ministry of Education.

References

- [1] S. Nakamura, M. Senoh, S. Nagahama, N. Iwasa, T. Yamada, T. Matsushita, H. Kiyoku, Y. Sugimoto, T. Kozaki, H. Umemoto, M. Sano, K. Chocho, *Appl. Phys. Lett.* 72 (2) (1998) 211.
- [2] S. Dalmaso, E. Feltin, P. de Mierry, B. Beaumont, P. Gibart, M. Leroux, *Electron. Lett.* 36 (2000) 1728.
- [3] J.W. Yang, A. Lunev, G. Simin, A. Chitnis, M. Shatalov, M. Asif Khan, J.E. Van Nostrand, R. Gaska, *Appl. Phys. Lett.* 76 (2000) 273.
- [4] J.K. Kim, J.L. Lee, *Electrochem. Soc.* 51 (3) (2004) G190–G195.
- [5] T. Egawa, N. Nakada, H. Ishikawa, M. Umeno, *Electron. Lett.* 36 (2000) 1816.
- [6] E. Feltin, B. Beaumont, M. Laügt, P. de Mierry, P. Vennèguès, H. Lahrèche, M. Leroux, P. Gibart, *Appl. Phys. Lett.* 79 (2001) 3230.
- [7] S. Nakamura, *Jpn. J. Appl. Phys.* 30 (1991) L17095.
- [8] H. Amano, N. Sawaki, I. Akasaki, Y. Toyoda, *Appl. Phys. Lett.* 48 (5) (1986) 353.
- [9] S. Tomiya, K. Funato, T. Asatsuma, T. Hino, S. Kijima, T. Asano, M. Ikeda, *Appl. Phys. Lett.* 77 (2000) 636.
- [10] J.S. Ha, S.W. Lee, H.J. Lee, H.J. Lee, S.H. Lee, H. Goto, T. Kato, K. Fujii, M.W. Cho, T. Yao, *IEEE Photonics Technol. Lett.* 20 (2008) 175.
- [11] H. Goto, S.W. Lee, H.J. Lee, J.S. Ha, M.W. Cho, T. Yao, *Phys. Stat. Sol. (C)* 5 (2008) 1659.
- [12] W.H. Lee, I.H. Im, T. Minegishi, T. Hanada, M.W. Cho, T. Yao, *J. Korean Phys. Soc.* 49 (3) (2006) 928.
- [13] W.H. Lee, S.W. Lee, H. Goto, H.C. Ko, M.W. Cho, T. Yao, *Phys. Stat. Sol. (C)* 3 (6) (2006) 1388–1391.
- [14] J.S. Ha, H.J. Lee, S.W. Lee, H.J. Lee, S.H. Lee, H. Goto, M.W. Cho, T. Yao, S.K. Hong, R. Toba, J.W. Lee, J.Y. Lee, *Appl. Phys. Lett.* 92 (2008) 091906.
- [15] C.W. Zou, H.J. Wang, M. Li, C.S. Liu, L.P. Guo, D.J. Fu, *Vacuum* 83 (2009) 1086.
- [16] T.V. Cuong, H.S. Cheong, H.G. Kim, C.H. Hong, E.K. Suh, H.K. Cho, B.H. Kong, *Appl. Phys. Lett.* 90 (2007) 131107.
- [17] W. Li, A.Z. Li, M. Oi, Y.G. Zhang, Z.B. Zhao, Q.K. Yang, *Mater. Sci. Eng. B: Solid B* 75 (2000) 224–227.
- [18] Jörg Neugebauer, G. Chris, Van de Walle, *Appl. Phys. Lett.* 69 (1996) 503.